

# Imitation Learning by State-Only Distribution Matching

Damian Boborzi<sup>\*1</sup>, Christoph-Nikolas Straehle<sup>\*2</sup>, Jens S. Buchner<sup>3</sup> and Lars Mikelsons<sup>1</sup>

<sup>1</sup>Augsburg University

<sup>2</sup>Bosch Center for Artificial Intelligence

<sup>3</sup>ETAS GmbH

damian.boborzi@uni-a.de

## Abstract

Imitation Learning from observation describes policy learning in a similar way to human learning. An agent’s policy is trained by observing an expert performing a task. While many state-only imitation learning approaches are based on adversarial imitation learning, one main drawback is that adversarial training is often unstable and lacks a reliable convergence estimator. If the true environment reward is unknown and cannot be used to select the best-performing model, this can result in bad real-world policy performance. We propose a non-adversarial learning-from-observations approach, together with an interpretable convergence and performance metric.

Our training objective minimizes the Kulback-Leibler divergence (KLD) between the policy and expert state transition trajectories which can be optimized in a non-adversarial fashion. Such methods demonstrate improved robustness when learned density models guide the optimization. We further improve the sample efficiency by rewriting the KLD minimization as the Soft Actor Critic objective based on a modified reward using additional density models that estimate the environment’s forward and backward dynamics. Finally, we evaluate the effectiveness of our approach on well-known continuous control environments and show state-of-the-art performance while having a reliable performance estimator compared to several recent learning-from-observation methods.

## 1 INTRODUCTION

Imitation learning (IL) describes methods that learn optimal behavior that is represented by a collection of expert demonstrations. While in standard reinforcement learning (RL), the agent is trained on environment feedback using a reward signal, IL can alleviate the problem of designing effective reward functions. This is particularly useful for tasks where demonstrations are more accessible than designing a reward function. One popular example is to train traffic agents in

a simulation to mimic real-world road users [Kuefler *et al.*, 2017].

Learning-from-demonstrations (LfD) describes IL approaches that require state-action pairs from expert demonstrations [Ho and Ermon, 2016]. While actions can guide policy learning, it might be very costly or even impossible to collect actions alongside state demonstrations in many real-world setups. For example, when expert demonstrations are available as video recordings without additional sensor signals. One example of such a setup is training traffic agents in a simulation, where the expert data contains recordings of traffic in bird’s eye view [Kuefler *et al.*, 2017]. No direct information on the vehicle physics, throttle, and steering angle is available. Another example is teaching a robot to pick, move, and place objects based on human demonstrations [Osa *et al.*, 2018]. In such scenarios, actions have to be estimated based on sometimes incomplete information to train an agent to imitate the observed behavior.

Alternatively, learning-from-observations (LfO) performs state-only IL and trains an agent without actions being available in the expert dataset [Torabi *et al.*, 2019]. While LfO is a more challenging task than LfD, it can be more practical in case of incomplete data sources. Learning an additional environment model may help to infer actions based on expert observations and the learned environment dynamics [Torabi *et al.*, 2018a]. Like LfD, distribution matching based on an adversarial setup is commonly used in LfO [Torabi *et al.*, 2018b]. In adversarial imitation learning (AIL), a policy is trained using an adversarial discriminator, which is used to estimate a reward that guides policy training. While AIL methods obtain better performing agents than supervised methods like behavioral cloning (BC) using less data, adversarial training often has stability issues [Miyato *et al.*, 2018] and under some conditions is not guaranteed to converge [Jin *et al.*, 2020]. Additionally, estimating the performance of a trained policy without access to the environment reward can be very challenging. While the duality gap [Gnarova *et al.*, 2019; Sidheekh *et al.*, 2021] is a convergence metric suited for GAN based methods, it is difficult to use in the AIL setup since it relies on the gradient of the generator for an optimization process. In the AIL setup, the generator consists of the policy and the environment and therefore the gradient is difficult to estimate with black box environments. As an alternative for AIL setups the predicted reward (discriminator

<sup>\*</sup>Both Authors contributed equally

output) or the policy loss can be used to estimate the performance.

To address the limitations of AIL, we propose a state-only distribution matching method that learns a policy in a non-adversarial way. We optimize the Kulback-Leibler divergence (KLD) between the actionless policy and expert trajectories by minimizing the KLD of the conditional state transition distribution of the policy and the expert for all time steps. We estimate the expert state transition distribution using normalizing flows, which can be trained offline using the expert dataset. Thus, stability issues arising from the min-max adversarial optimization in AIL methods can be avoided. This objective is similar to FORM [Jaegle *et al.*, 2021], which was shown to be more stable in the presence of task-irrelevant features.

While maximum entropy RL methods [Ziebart, 2010] can improve policy training by increasing the exploration of the agent, they also add a bias if being used to minimize the proposed KLD. To match the transition distributions of the policy and the expert exactly, the state-next-state distribution of the policy is expanded into policy entropy, forward dynamics and inverse action model of the environment. It has been shown that such dynamic models can improve the convergence [Zhu *et al.*, 2020] and are well suited to infer actions not available in the dataset [Torabi *et al.*, 2018a]. We model these distributions using normalizing flow models which have been demonstrated to perform very well on learning complex probability distributions [Papamakarios *et al.*, 2019]. Combining all estimates results in an interpretable reward that can be used together with standard maximum entropy RL methods [Haarnoja *et al.*, 2018a]. The optimization based on the KLD provides a reliable convergence metric of the training and a good estimator for policy performance.

As contributions we derive SOIL-TDM (State Only Imitation Learning by Trajectory Distribution Matching), a non-adversarial LfO method which minimizes the KLD between the conditional state transition distributions of the policy and the expert using maximum entropy RL. We show the convergence of the proposed method using off-policy samples from a replay buffer. We develop a practical algorithm based on the SOIL-TDM objective and demonstrate its effectiveness to measure its convergence compared to several other state-of-the-art methods. Empirically we compared our method to the recent state-of-the-art IL approaches OPOLO [Zhu *et al.*, 2020], f-IRL [Ni *et al.*, 2020], and FORM [Jaegle *et al.*, 2021] in complex continuous control environments. We demonstrate that our method is superior especially if the selection of the best policy cannot be based on the true environment reward signal. This is a setting which more closely resembles real-world applications in autonomous driving or robotics where it is difficult to define a reward function [Osa *et al.*, 2018].

## 2 Background

In this work, we want to train a stochastic policy function  $\pi_\theta(a_t|s_t)$  in continuous action spaces with parameters  $\theta$  in a sequential decision making task considering finite-

horizon environments<sup>1</sup>. The problem is modeled as a Markov Decision Process (MDP), which is described by the tuple  $(S, A, p, r)$  with the continuous state spaces  $S$  and action spaces  $A$ . The transition probability is described by  $p(s_{t+1}|s_t, a_t)$  and the bounded reward function by  $r(s_t, a_t)$ . At every time step  $t$  the agent interacts with its environment by observing a state  $s_t$  and taking an action  $a_t$ . This results in a new state  $s_{t+1}$  and a reward signal  $r_{t+1}$  based on the transition probability and reward function. We will use  $\mu^{\pi_\theta}(s_t, a_t)$  to denote the state-action marginals at time step  $t$  of the trajectory distribution induced by the policy  $\pi_\theta(a_t|s_t)$ .

### 2.1 Maximum Entropy Reinforcement Learning and Soft Actor Critic

The standard objective in RL is the expected sum of undiscounted rewards  $\sum_{t=0}^T \mathbb{E}_{(s_t, a_t) \sim \mu^{\pi_\theta}} [r(s_t, a_t)]$ . The goal of the agent is to learn a policy  $\pi_\theta(a_t|s_t)$  which maximises this objective. The maximum entropy objective

$$J(\pi_\theta) = \sum_{t=0}^T \mathbb{E}_{(s_t, a_t) \sim \mu^{\pi_\theta}} [r(s_t, a_t) + \alpha \mathcal{H}(\pi_\theta(\cdot|s_t))] \quad (1)$$

introduces a modified goal for the RL agent, where the agent has to maximise the sum of the reward signal and its output entropy  $\mathcal{H}(\pi_\theta(\cdot|s_t))$  [Ziebart, 2010]. The parameter  $\alpha$  controls the stochasticity of the optimal policy by determining the relative importance of the entropy term versus the reward.

Soft Actor-Critic (SAC) [Haarnoja *et al.*, 2018a; Haarnoja *et al.*, 2018b] combines off-policy Q-Learning with a stable stochastic actor-critic formulation. The soft Q-function parameters  $\Psi$  can be trained with:

$$J_Q = \mathbb{E}_{(s_t, a_t) \sim D_{RB}} \left[ \frac{1}{2} (Q_\Psi(s_t, a_t) - (r(s_t, a_t) + \gamma \mathbb{E}_{s_{t+1}} [V_{\hat{\Psi}}(s_{t+1})]))^2 \right] \quad (2)$$

The soft state value function is defined by:

$$V^\pi(s_t) := \mathbb{E}_{a_t \sim \pi} [Q(s_t, a_t) - \alpha \log \pi_\theta(a_t|s_t)] \quad (3)$$

Lastly, the policy is optimized by minimizing the following objective:

$$J_\pi = \mathbb{E}_{(s_t) \sim D_{RB}} [\mathbb{E}_{(a_t) \sim \pi_\theta} [\alpha \log \pi_\theta(a_t|s_t) - Q_\Psi(s_t, a_t)]] \quad (4)$$

### 2.2 Imitation Learning

In the IL setup, the agent does not have access to the true environment reward function  $r(s_t, a_t)$  and instead has to imitate expert trajectories performed by an expert policy  $\pi_E$  collected in a dataset  $\mathcal{D}_E$ .

In the typical **learning-from-demonstration** setup the expert demonstrations  $\mathcal{D}_E^{LfD} := \{s_t^k, a_t^k, s_{t+1}^k\}_{k=1}^N$  are given by action-state-next-state transitions. Distribution matching has been a popular choice among different LfD approaches. The policy  $\pi_\theta$  is learned by minimizing the discrepancy between the stationary state-action distribution induced by the expert  $\mu^E(s, a)$  and the policy  $\mu^{\pi_\theta}(s, a)$ . An overview and comparison of different LfD objectives resulting from this discrepancy minimization was done by Ghasemipour *et al.* [2019].

<sup>1</sup>An extension to infinite-horizons is given in section 3

Often the backward KLD is used to measure this discrepancy [Fu *et al.*, 2017]:

$$\min J_{LFD}(\pi_\theta) := \min \mathbb{D}_{KL}(\mu^{\pi_\theta}(s, a) || \mu^E(s, a)) \quad (5)$$

**Learning-from-observation** (LfO) considers a more challenging task where expert actions are not available. Hence, the demonstrations  $\mathcal{D}_E^{LfO} := \{s_t^k, s_{t+1}^k\}_{k=1}^N$  consist of state-next-state transitions. The policy learns which actions to take based on interactions with the environment and the expert state transitions. Distribution matching based on state-transition distributions is a popular choice for state-only IL [Torabi *et al.*, 2018b; Zhu *et al.*, 2020]:

$$\min J_{LfO}(\pi_\theta) := \min \mathbb{D}_{KL}(\mu^{\pi_\theta}(s, s') || \mu^E(s, s')) \quad (6)$$

### 3 Method

In a finite horizon MDP setting, the joint state-only trajectory distributions are defined by the start state distribution  $p(s_0)$  and the product of the conditional state transition distributions  $p(s_{i+1}|s_i)$ . For the policy distribution  $\mu^{\pi_\theta}$  and the expert distribution  $\mu^E$  this becomes:

$$\mu^{\pi_\theta}(s_T, \dots, s_0) = p(s_0) \prod_{i=0..T-1} \mu^{\pi_\theta}(s_{i+1}|s_i),$$

$$\mu^E(s_T, \dots, s_0) = p(s_0) \prod_{i=0..T-1} \mu^E(s_{i+1}|s_i)$$

Our goal is to match the state-only trajectory distribution  $\mu^{\pi_\theta}$  induced by the policy with the state-only expert trajectory distribution  $\mu^E$  by minimizing the Kulback-Leibler divergence (KLD) between them:

$$\begin{aligned} J_{SOIL-TDM} &= \mathbb{D}_{KL}(\mu^{\pi_\theta} || \mu^E) \\ &= \mathbb{E}_{(s_T, \dots, s_0) \sim \mu^{\pi_\theta}} [\log \mu^{\pi_\theta} - \log \mu^E] \\ &= \sum_{i=0..T-1} \mathbb{E}_{(s_{i+1}, s_i) \sim \mu^{\pi_\theta}} [\log \mu^{\pi_\theta}(s_{i+1}|s_i) \\ &\quad - \log \mu^E(s_{i+1}|s_i)] \end{aligned} \quad (7)$$

The conditional expert state transition distribution  $\mu^E(s_{i+1}|s_i)$  can be learned offline from the demonstrations for example by training a conditional normalizing flow on the given state/next-state pairs. The policy induced conditional state transition distribution can be rewritten with the Bayes theorem using the environment model  $p(s_{i+1}|a_i, s_i)$  and the inverse action distribution density  $\pi'_\theta(a_i|s_{i+1}, s_i)$ :

$$\mu^{\pi_\theta}(s_{i+1}|s_i) = \frac{p(s_{i+1}|a_i, s_i)\pi_\theta(a_i|s_i)}{\pi'_\theta(a_i|s_{i+1}, s_i)} \quad (8)$$

It holds for any  $a_i$  where  $\pi' > 0$ . Thus, one can extend the expectation over  $(s_{i+1}, s_i)$  by the action  $a_i$  and the KLD minimization  $\min \mathbb{D}_{KL}(\mu^{\pi_\theta} || \mu^E)$  can be rewritten as

$$\begin{aligned} \min \sum_{i=0..T-1} \mathbb{E}_{(s_i, a_i, s_{i+1}) \sim \pi_\theta} [\log p(s_{i+1}|a_i, s_i) + \log \pi_\theta(a_i|s_i) \\ - \log \pi'_\theta(a_i|s_{i+1}, s_i) - \log \mu^E(s_{i+1}|s_i)] \end{aligned} \quad (9)$$

Now, by defining a reward function (also see A.2)

$$\begin{aligned} r(a_i, s_i) := &\mathbb{E}_{s_{i+1} \sim p(s_{i+1}|a_i, s_i)} [-\log p(s_{i+1}|a_i, s_i) \\ &+ \log \pi'_\theta(a_i|s_{i+1}, s_i) + \log \mu^E(s_{i+1}|s_i)] \end{aligned} \quad (10)$$

that depends on the expert state transition likelihood  $\mu^E(s_{i+1}|s_i)$ , on the environment model  $p(s_{i+1}|a_i, s_i)$  and on the inverse action distribution density  $\pi'_\theta(a_i|s_{i+1}, s_i)$ . The state-only trajectory distribution matching problem can be transformed to a max-entropy RL task:

$$\begin{aligned} \min \mathbb{D}_{KL}(\mu^{\pi_\theta} || \mu^E) \\ = \max \sum_{i=0..T-1} \mathbb{E}_{(a_i, s_i) \sim \pi_\theta} [-\log \pi_\theta(a_i|s_i) + r(a_i, s_i)] \\ = \max \sum_{i=0..T-1} \mathbb{E}_{(a_i, s_i) \sim \pi_\theta} [r(a_i, s_i) + \mathcal{H}(\pi_\theta(\cdot|s))] \end{aligned} \quad (11)$$

In practice the reward function  $r(a_i, s_i)$  can be computed using monte carlo integration with a single sample from  $p(s_{i+1}|a_i, s_i)$  using the replay buffer.

This max-entropy RL task can be optimized with standard max-entropy RL algorithms. In this work, we applied the SAC algorithm [Haarnoja *et al.*, 2018a] as it is outlined in Section 2.1.

The extension to infinite horizon tasks can be done by introducing a discount factor  $\gamma$  as in the work by Haarnoja *et al.* [2018b]. In combination with our reward definition one obtains the following infinite horizon maximum entropy objective:

$$\begin{aligned} J_{ME-iH} = \sum_{i=0..inf} \mathbb{E}_{(a_i, s_i) \sim \pi_\theta} \left[ \sum_{j=i..inf} \gamma^{j-i} \right. \\ \left. \mathbb{E}_{(a_j, s_j) \sim \pi_\theta} [r(a_j, s_j) + \mathcal{H}(\pi_\theta(\cdot|s_j)|s_i, a_i)] \right] \end{aligned} \quad (12)$$

#### 3.1 Algorithm

To evaluate the reward function, the environment model  $p(s_{i+1}|a_i, s_i)$  and the inverse action distribution function  $\pi'_\theta(a_i|s_{i+1}, s_i)$  have to be estimated. We model both distributions using conditional normalizing flows and train with maximum likelihood based on expert demonstrations and rollout data from a replay buffer. The environment model  $p(s_{i+1}|a_i, s_i)$  is modeled by  $\mu_\phi(s_{i+1}|a_i, s_i)$  with parameter  $\phi$  and the inverse action distribution function  $\pi'_\theta(a_i|s_{i+1}, s_i)$  is modeled by  $\mu_\eta(a_i|s_{i+1}, s_i)$  with parameter  $\eta$ .

The whole training process according to Algorithm 1 is described in the following<sup>2</sup>. The expert state transition model  $\mu^E(s_{t+1}|s_t)$  is trained offline using the expert dataset  $D_E$  which contains  $K$  expert state trajectories. We assume the expert distribution is correctly represented by the dataset. Density modeling of the expert state transitions can still result in overfitting when only few expert demonstrations are available (in the few sample limit). We improved the expert training process by adding Gaussian noise to the state values. The standard deviation of the noise is reduced during training so that the model has a correct estimate of the density without

<sup>2</sup>Code will be available at [https://github.com/\\*](https://github.com/*)

overfitting to the explicit demonstrations. With this approach we are able to successfully train expert state transition models on as few as one expert trajectory. The influence of this improved routine is studied in Appendix A.6. After this initial step the following process is repeated until convergence in each episode. The policy interacts with the environment for  $T$  steps to collect state-action-next-state information, which is saved in the replay buffer  $D_{RB}$ . The conditional normalizing flows for the environment model  $\mu_\phi(s_{i+1}|a_i, s_i)$  (policy independent) and the inverse action distribution model  $\mu_\eta(a_i|s_{i+1}, s_i)$  (policy dependent) are optimized using samples from the replay buffer  $D_{RB}$  for  $N$  steps. In Appendix A.3 we show that this reduces the KLD (Equation 9) in each step. Afterwards we use the learned models together with the samples from the replay buffer to compute a one-sample monte carlo approximation of the reward to train the Q-function. The policy  $\pi_\theta(a_t|s_t)$  is updated using SAC. The SAC-based Q-function training and policy optimization also minimize Equation 9 (see Equation 11) in each step. Together with the inverse action policy learning they lead to a converging algorithm since all steps reduce the KLD, which is bounded from below by 0. It is worth noting that the overall algorithm is non-adversarial, the inverse action policy optimization and the policy optimization using SAC both reduce the overall objective - the KLD. Contrary to AIL algorithms like OPOLO, it is not based on an adversarial nested min-max optimization. Additionally, we can estimate the similarity of state transitions from our policy to the expert during each optimization step, since we model all densities in the rewritten KLD from Equation 9. As a result we have a reliable performance estimate enabling us to select the best performing policy based on the lowest KLD between policy and expert state transition trajectories.

### 3.2 Relation to learning from observations

The LfO objective of previous approaches like OPOLO minimizes the divergence between the joint policy state transition distribution and the joint expert state transition distribution:

$$J_{LfO} = \mathbb{D}_{KL}(\mu^{\pi_\theta}(s', s) || \mu^E(s', s)) \quad (13)$$

which can be rewritten as (see A.1)

$$J_{LfO} = \mathbb{D}_{KL}(\mu^{\pi_\theta}(s_T, \dots, s_0) || \mu^E(s_T, \dots, s_0)) + \sum_{i=1..T-1} \mathbb{D}_{KL}(\mu^{\pi_\theta}(s_i) || \mu^E(s_i)) \quad (14)$$

Thus, this LfO objective minimizes the sum of the KLD between the joint distributions and the KLDs of the marginal distributions. The SOIL-TDM objective in comparison minimizes purely the KLD of the joint distributions. In case of a perfect distribution matching - a zero KLD between the joint distributions - the KLDs of the marginals also vanish so both objectives have the same optimum.

## 4 Related Work

Many recent IL approaches are based on inverse RL (IRL) [Ng and Russell, 2000]. In IRL, the goal is to learn a reward signal for which the expert policy is optimal. AIL algorithms

---

### Algorithm 1 State-Only Imitation Learning by Trajectory Distribution Matching (SOIL-TDM)

---

```

1: procedure SOIL-TDM( $D_E$ )
2:   Train  $\mu^E(s_{t+1}|s_t)$  with  $D_E : \{s_0, s_1, \dots, s_T\}_{k=0}^K$ 
3:   for episodes do
4:     for range( $T$ ) do ▷ generate data
5:        $\hat{a}_t \leftarrow \text{sample}(\pi_\theta(\hat{a}_t|s_t))$ 
6:        $s_{t+1} \leftarrow p_{sim}(s_{t+1}|s_t, \hat{a}_t)$  ▷ apply action
7:       Store  $(s_t, \hat{a}_t, s_{t+1})$  in  $D_{RB}$ 
8:     end for
9:     for range( $N$ ) do ▷ update dynamics models
10:       $\{(s_t, \hat{a}_t, s_{t+1})\}_{i=1}^B \sim D_{RB}$  ▷ sample batch
11:      train  $\mu_\eta(\hat{a}_t|s_{t+1}, s_t)$  and  $\mu_\phi(s_{t+1}|\hat{a}_t, s_t)$ 
12:    end for
13:    for range( $N$ ) do ▷ SAC Optimization
14:       $\{(s_t, \hat{a}_t, s_{t+1})\}_{i=1}^B \sim D_{RB}$  ▷ sample batch
15:       $a_t \leftarrow \text{sample}(\pi_\theta(a_t|s_t))$ 
16:      optimize  $\pi_\theta(a_t|s_t)$  with  $J_\pi$  from eq. 4
17:      ▷ estimate reward
18:       $r(s_t, \hat{a}_t) \leftarrow -\log \mu_\phi(s_{t+1}|\hat{a}_t, s_t) +$ 
19:       $\log \mu_\eta(\hat{a}_t|s_{t+1}, s_t) + \log \mu^E(s_{t+1}|s_t)$ 
20:      optimize  $Q_\psi(\hat{a}_t, s_t)$  with  $J_Q$  from eq. 2
21:    end for
22:  end procedure

```

---

are popular methods to perform IL in a RL setup [Ho and Ermon, 2016; Fu *et al.*, 2017; Kostrikov *et al.*, 2020]. In AIL, a discriminator gets trained to distinguish between expert states and states coming from policy rollouts. The goal of the policy is to fool the discriminator. The policy gets optimized to match the state action distribution of the expert, using this two-player game. Based on this idea more general approaches have been derived based on f-divergences. Ni *et al.*[2020] derive an analytic gradient of any f-divergence between the agent and expert state distribution w.r.t. reward parameters. Based on this gradient they present the algorithm f-IRL that recovers a stationary reward function from the expert density by gradient descent. Ghasemipour *et al.*[2019] identify that IRL’s state-marginal matching objective contributes most to its superior performance and apply this understanding to teach agents a diverse range of behaviours using simply hand-specified state distributions.

A key problem with AIL for LfD and LfO is optimization instability [Miyato *et al.*, 2018]. Wang *et al.*[2019] avoid the instabilities resulting from adversarial optimization by estimating the support of the expert policy to compute a fixed reward function. Similarly, Brantley *et al.*[2020] use a fixed reward function by estimating the variance of an ensemble of policies. Both methods rely on additional behavioral cloning steps to reach expert-level performance. Liu *et al.*[2020] propose Energy-Based Imitation Learning (EBIL) which recovers fixed and interpretative reward signals by directly estimating the expert’s energy. Neural Density Imitation (NDI) [Kim *et al.*, 2021] uses density models to perform distribution matching. Deterministic and Discriminative Imitation (D2-Imitation) [Sun *et al.*, 2021] requires no adver-

serial training by partitioning samples into two replay buffers and then learning a deterministic policy via off-policy reinforcement learning. Inverse soft-Q learning (IQ-Learn) [Garg *et al.*, 2021] avoids adversarial training by learning a single Q-function to implicitly representing both reward and policy. The implicitly learned rewards from IQ-Learn show a high positive correlation with the ground-truth rewards.

LfO can be divided into model-free and model-based approaches. GAILfO [Torabi *et al.*, 2018b] is a model-free approach which uses the GAIL principle with the discriminator input being state-only. Yang *et al.* [2019] analyzed the gap between the LfD and LfO objectives and proved that it lies in the disagreement of inverse dynamics models between the imitator and expert. Their proposed method IDDM is based on an upper bound of this gap in a model-free way. OPOLO [Zhu *et al.*, 2020] is a sample-efficient LfO approach also based on AIL, which enables off-policy optimization. The policy update is also regulated with an inverse action model that assists distribution matching in a mode-covering perspective.

Other model-based approaches either apply forward dynamics models or inverse action models. Sun *et al.* [2019] proposed a solution based on forward dynamics models to learn time dependant policies. While being provably efficient, it is not suited for infinite horizon tasks. Alternatively, behavior cloning from observations (BCO) [Torabi *et al.*, 2018a] learns an inverse action model based on simulator interactions to infer actions based on the expert state demonstrations. GPRIL [Schroecker *et al.*, 2019] uses normalizing flows as generative models to learn backward dynamics models to estimate predecessor transitions and augmenting the expert data set with further trajectories, which lead to expert states. Jiang *et al.* [2020] investigated IL using few expert demonstrations and a simulator with misspecified dynamics. A detailed overview of LfO was done by Torabi *et al.* [2019].

#### 4.1 Method Discussion and Relation to FORM

While our proposed method SOIL-TDM was independently developed it is most similar to the state-only approach FORM [Jaegle *et al.*, 2021]. In FORM the policy training is guided by a conditional density estimation of the expert’s observed state transitions. In addition a state transition model  $\mu_{\Phi}^{\pi^{\theta}}(s_{i+1}|s_i)$  of the current policy is learned. The policy reward is estimated by:  $r_i = \log\mu^E(s_{i+1}|s_i) - \log\mu_{\Phi}^{\pi^{\theta}}(s_{i+1}|s_i)$ . The approach matches conditional state transition probabilities of expert and policy in comparison to the joint state-action (like GAIL) or joint state-next-state (like OPOLO or GAILfO) densities. The authors argue that this has consequences in the robustness of the different approaches. Namely, methods based on conditional state probabilities are less sensitive to erroneously penalizing features that may not be in the demonstrator data but lead to correct transitions. Hence, such methods may be less prone to overfit to irrelevant differences. Jaegle *et al.* [2021] demonstrate the benefit of such a conditional density matching approach.

In contrast to FORM we show in Equation 8 that the policies next-state conditional density  $\mu^{\pi^{\theta}}(s_{i+1}|s_i)$  can be separated into the policies action density and the forward- and the backward-dynamics densities. Using this decomposition

we show that the KLD minimization is equivalent to a maximum entropy RL objective (see Equation 9) with a special reward (see Equation 10). Here the entropy of the policy stemming from the decomposition of the conditional state-next-state density leads to the maximum entropy RL objective. Jaegle *et al.* [2021] mention that the second term in their reward objective can be viewed as an entropy-like expression. Hence, if this reward is optimized using a RL algorithm which includes some form of policy entropy regularization this entropy is basically weighted twice. In the experiments we show that this double accounting of the policy entropy negatively affects the sample efficiency of the algorithm in comparison to our method.

## 5 Experiments

We evaluate our proposed method described in Section 3 in a variety of different IL tasks and compare it against the baseline methods OPOLO, F-IRL and FORM. We evaluate and compare all methods in complex and high dimensional continuous control environments using the Pybullet physics simulation [Coumans and Bai, 2016 2019]. To evaluate the performance of all methods, the episode rewards of the trained policies are compared to reward from the expert policy. The expert data generation as well as the used baseline implementations are described in Appendix A.5.

Since we assume no environment reward is available as an early stopping criterion, we use other convergence estimates available during training to select the best policy for each method. In adversarial training the duality gap [Grnarova *et al.*, 2019; Sidheekh *et al.*, 2021] is an established method to estimate the convergence of the training process. In the IL setup the duality gap can be very difficult to estimate since it requires the gradient of the policy and the environment (i.e. the gradient of the generator) for the optimization process it relies on. We therefore use two alternatives for model selection for OPOLO. The first approach selects the model with the lowest policy loss and the second approach selects the model based on the highest estimated reward over ten consecutive epochs. For F-IRL we selected the model with the lowest estimated Jensen-Shannon divergence over ten epochs. To estimate the convergence of SOIL-TDM the policy loss based on the KLD from equation 9 is used. It can be estimated using the same models used for training the policy. Similarly, we used the effect models of FORM to estimate the convergence based on the reward.

The evaluation is done by running 3 training runs with ten test episodes (in total 30 rollouts) for each trained policy and calculating the respective mean and confidence interval for all runs. We plot the rewards normalized so that 1 corresponds to expert performance. Values above 1 mean that the agent has achieved a higher reward than the mean of the expert (episode rewards of the expert are reported in Appendix A.5). Implementation details of our method are described in Appendix A.4.

The evaluation results of the discussed methods on a suite of continuous control tasks with unknown true environment reward as a selection criterion are shown in Figure 1. The achieved rewards are plotted with respect to the number of

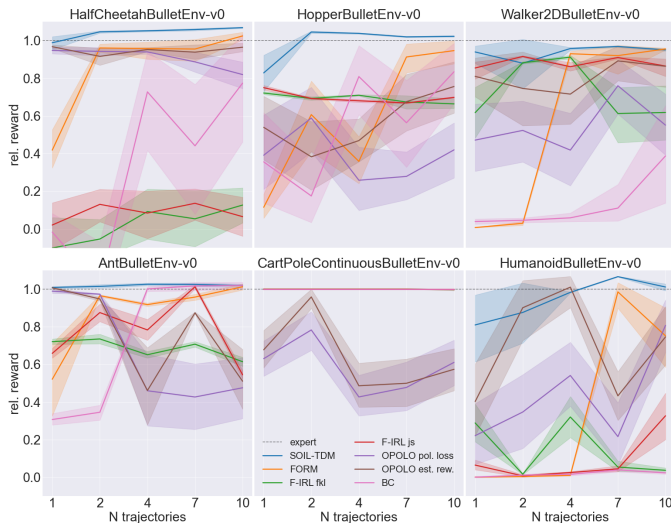


Figure 1: Unknown true environment reward selection criteria: Relative reward for different amount of expert trajectories on continuous control environments. The best policies based on estimated convergence values were selected. The value 1 corresponds to expert policy performance.

expert trajectories provided for training the agent. The confidence intervals are plotted using lighter colors.

If the true environment reward is unknown the results show that SOIL-TDM achieves or surpasses the performance of the baseline methods on all tested environments (with the exception of two and four expert trajectories in the HumanoidBulletEnv-v0 environment and two trajectories in the Walker2DBulletEnv-v0 environment). In general the adversarial based methods OPOLO and F-IRL exhibit a high variance of the achieved rewards using the proposed selection criteria. While loss and reward are well suited for selecting the best model in usual setups, the results demonstrate that they might be less expressive for estimating the convergence in adversarial training due to the min-max game of the discriminator and the policy. The stability of the SOIL-TDM training method is evident from the small confidence band of the results which gets smaller for more expert demonstrations. While the selection of FORM is also more stable compared to the adversarial methods it generally achieves lower rewards in the sample efficient regime of one and two expert trajectories.

Figure 2 shows the benchmark results of OPOLO, F-IRL, FORM, and SOIL-TDM if the true environment reward is used as an early stopping criterion. In this setup, our method still achieves competitive performance or surpasses OPOLO, F-IRL, and FORM. Additional figures for a comparison of the training performance and efficiency can be found in the Appendix A.7. An ablation study for our method is in the Appendix A.6.

## 6 Conclusion

In this work we propose a non-adversarial state-only imitation learning approach based on the minimization of the

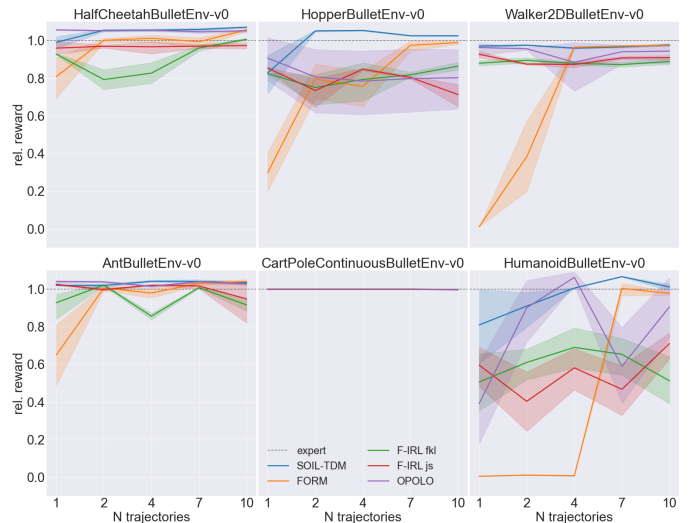


Figure 2: Best true environment reward selection criterion: Relative reward for different amount of expert trajectories on continuous control environments. The value 1 corresponds to expert policy performance.

Kulback-Leibler divergence between the policy and the expert state trajectory distribution. This objective leads to a maximum entropy reinforcement learning problem with a reward function depending on the expert state transition distribution and the forward and backward dynamics of the environment which can be modeled using conditional normalizing flows. The proposed approach is compared to several state-of-the-art learning from observations methods in a scenario with unknown environment rewards and achieves state-of-the-art performance.

## References

- [Ardizzone *et al.*, 2019] Lynton Ardizzone, Jakob Kruse, Carsten Rother, and Ullrich Köthe. Analyzing inverse problems with invertible neural networks. In *International Conference on Learning Representations, ICLR*, 2019.
- [Brantley *et al.*, 2020] Kiante Brantley, Wen Sun, and Mikael Henaff. Disagreement-regularized imitation learning. In *International Conference on Learning Representations, ICLR*, 2020.
- [Coumans and Bai, 2016 2019] Erwin Coumans and Yunfei Bai. Pybullet, a python module for physics simulation for games, robotics and machine learning. <http://pybullet.org>, 2016–2019.
- [Dinh *et al.*, 2017] Laurent Dinh, Jascha Sohl-Dickstein, and Samy Bengio. Density estimation using real nvp, 2017.
- [Fu *et al.*, 2017] Justin Fu, Katie Luo, and Sergey Levine. Learning robust rewards with adversarial inverse reinforcement learning. In *International Conference on Learning Representations, ICLR*, 2017.
- [Garg *et al.*, 2021] Divyansh Garg, Shuvam Chakraborty, Chris Cundy, Jiaming Song, and Stefano Ermon. IQ-learn: Inverse soft-q learning for imitation. In *Thirty-Fifth Conference on Neural Information Processing Systems*, 2021.
- [Ghasemipour *et al.*, 2019] Seyed Kamyar Seyed Ghasemipour, Richard S. Zemel, and Shixiang Gu. A divergence minimization perspective on imitation learning methods. In *3rd Annual*

- Conference on Robot Learning, CoRL*, Proceedings of Machine Learning Research, 2019.
- [Grnarova *et al.*, 2019] Paulina Grnarova, Kfir Y. Levy, Aurelien Lucchi, Nathanael Perraudin, Ian Goodfellow, Thomas Hofmann, and Andreas Krause. A domain agnostic measure for monitoring and evaluating gans. In *Advances in Neural Information Processing Systems*, 2019.
- [Haarnoja *et al.*, 2018a] Tuomas Haarnoja, Aurick Zhou, Pieter Abbeel, and Sergey Levine. Soft actor-critic: Off-policy maximum entropy deep reinforcement learning with a stochastic actor. In *Proceedings of the 35th International Conference on Machine Learning*, 2018.
- [Haarnoja *et al.*, 2018b] Tuomas Haarnoja, Aurick Zhou, Kristian Hartikainen, George Tucker, Sehoon Ha, Jie Tan, Vikash Kumar, Henry Zhu, Abhishek Gupta, Pieter Abbeel, and Sergey Levine. Soft actor-critic algorithms and applications. Technical report, 2018.
- [Ho and Ermon, 2016] Jonathan Ho and Stefano Ermon. Generative adversarial imitation learning. In *Advances in Neural Information Processing Systems*. Curran Associates, Inc., 2016.
- [Jaegle *et al.*, 2021] Andrew Jaegle, Yury Sulsky, Arun Ahuja, Jake Bruce, Rob Fergus, and Greg Wayne. Imitation by predicting observations. In *Proceedings of the 38th International Conference on Machine Learning*, 2021.
- [Jiang *et al.*, 2020] Shengyi Jiang, Jingcheng Pang, and Yang Yu. Offline imitation learning with a misspecified simulator. In *Advances in Neural Information Processing Systems*, 2020.
- [Jin *et al.*, 2020] Chi Jin, Praneeth Netrapalli, and Michael Jordan. What is local optimality in nonconvex-nonconcave minimax optimization? In *Proceedings of the 37th International Conference on Machine Learning*, 2020.
- [Kim *et al.*, 2021] Kuno Kim, Akshat Jindal, Yang Song, Jiaming Song, Yanan Sui, and Stefano Ermon. Imitation with neural density models. In *arxiv:cs.LG*, 2021.
- [Kingma and Ba, 2015] Diederik P. Kingma and Jimmy Ba. Adam: A method for stochastic optimization. In *International Conference on Learning Representations, ICLR*, 2015.
- [Kingma and Dhariwal, 2018] Durk P Kingma and Prafulla Dhariwal. Glow: Generative flow with invertible 1x1 convolutions. In *Advances in Neural Information Processing Systems*, 2018.
- [Kostrikov *et al.*, 2020] Ilya Kostrikov, Ofir Nachum, and Jonathan Tompson. Imitation learning via off-policy distribution matching. In *International Conference on Learning Representations, ICLR*, 2020.
- [Kuefler *et al.*, 2017] Alex Kuefler, Jeremy Morton, Tim Wheeler, and Mykel Kochenderfer. Imitating driver behavior with generative adversarial networks. In *2017 IEEE Intelligent Vehicles Symposium (IV)*, 2017.
- [Liu *et al.*, 2020] Minghuan Liu, Tairan He, Minkai Xu, and Weinan Zhang. Energy-based imitation learning. *Autonomous Agents and Multi-Agent Systems*, 2020.
- [Miyato *et al.*, 2018] Takeru Miyato, Toshiki Kataoka, Masanori Koyama, and Yuichi Yoshida. Spectral normalization for generative adversarial networks. In *International Conference on Learning Representations, ICLR*, 2018.
- [Ng and Russell, 2000] A. Ng and S. Russell. Algorithms for inverse reinforcement learning. In *International Conference on Machine Learning*, 2000.
- [Ni *et al.*, 2020] Tianwei Ni, Harshit Sikchi, Yufei Wang, Tejus Gupta, Lisa Lee, and Ben Eysenbach. f-irl: Inverse reinforcement learning via state marginal matching. In *Conference on Robot Learning*, 2020.
- [Osa *et al.*, 2018] Takayuki Osa, Joni Pajarinen, Gerhard Neumann, J. Andrew Bagnell, Pieter Abbeel, and Jan Peters. An algorithmic perspective on imitation learning. In *Foundations and Trends in Robotics*, 2018.
- [Papamakarios *et al.*, 2019] George Papamakarios, Eric T. Nalisnick, Danilo Jimenez Rezende, Shakir Mohamed, and Balaji Lakshminarayanan. Normalizing flows for probabilistic modeling and inference. *Journal of Machine Learning Research*, 2019.
- [Schroeder *et al.*, 2019] Yannick Schroeder, Mel Vecerik, and Jonathan Scholz. Generative predecessor models for sample-efficient imitation learning. In *International Conference on Learning Representations, ICLR*, 2019.
- [Sidheekh *et al.*, 2021] Sahil Sidheekh, Aroof Aimen, Vineet Madan, and N. C. Krishnan. On duality gap as a measure for monitoring gan training. *2021 International Joint Conference on Neural Networks (IJCNN)*, 2021.
- [Sun *et al.*, 2019] Wen Sun, Anirudh Vemula, Byron Boots, and Drew Bagnell. Provably efficient imitation learning from observation alone. In *Proceedings of the 36th International Conference on Machine Learning*, 2019.
- [Sun *et al.*, 2021] Mingfei Sun, Sam Devlin, Katja Hofmann, and Shimon Whiteson. Deterministic and discriminative imitation (d2-imitation): Revisiting adversarial imitation for sample efficiency. In *Association for the Advancement of Artificial Intelligence*, 2021.
- [Torabi *et al.*, 2018a] Faraz Torabi, Garrett Warnell, and Peter Stone. Behavioral cloning from observation. In *Proceedings of the Twenty-Seventh International Joint Conference on Artificial Intelligence*, 2018.
- [Torabi *et al.*, 2018b] Faraz Torabi, Garrett Warnell, and Peter Stone. Generative adversarial imitation from observation. In *International Conference on Machine Learning Workshop on Imitation, Intent, and Interaction (I3)*, 2018.
- [Torabi *et al.*, 2019] Faraz Torabi, Garrett Warnell, and Peter Stone. Recent advances in imitation learning from observation. In *Proceedings of the Twenty-Eighth International Joint Conference on Artificial Intelligence*, 2019.
- [Wang *et al.*, 2019] Ruohan Wang, Carlo Ciliberto, Pierluigi Vito Amadori, and Yiannis Demiris. Random expert distillation: Imitation learning via expert policy support estimation. In *Proceedings of the 36th International Conference on Machine Learning*, 2019.
- [Yang *et al.*, 2019] Chao Yang, Xiaojian Ma, Wenbing Huang, Fuchun Sun, Huaping Liu, Junzhou Huang, and Chuang Gan. Imitation learning from observations by minimizing inverse dynamics disagreement. In *Advances in Neural Information Processing Systems*, 2019.
- [Zhu *et al.*, 2020] Zhuangdi Zhu, Kaixiang Lin, Bo Dai, and Jiayu Zhou. Off-policy imitation learning from observations. In *Advances in Neural Information Processing Systems*, 2020.
- [Ziebart, 2010] Brian D. Ziebart. *Modeling Purposeful Adaptive Behavior with the Principle of Maximum Causal Entropy*. PhD thesis, 2010.

## A Appendix

### A.1 Relation to LfO

The learning from observations (LfO) objective minimizes the divergence between the joint policy state transition distribution and the joint expert state transition distribution:

$$\min J_{LfO} = \min \mathbb{D}_{KL}(\mu^{\pi_\theta}(s', s) || \mu^E(s', s)) \quad (15)$$

where  $s'$  is a successor state of  $s$  given a stationary policy and stationary  $s', s$  marginals. This can be rewritten as

$$\begin{aligned} J_{LfO} &= \sum_{i=0..T-1} \mathbb{D}_{KL}(\mu^{\pi_\theta}(s_{i+1}, s_i) || \mu^E(s_{i+1}, s_i)) \\ &= \sum_{i=0..T-1} \int \mu^{\pi_\theta}(s_{i+1}, s_i) (\log \mu^{\pi_\theta}(s_{i+1}, s_i) \\ &\quad - \log \mu^E(s_{i+1}, s_i)) \\ &= \sum_{i=0..T-1} \int \mu^{\pi_\theta}(s_T, \dots, s_0) (\log \mu^{\pi_\theta}(s_{i+1}, s_i) \\ &\quad - \log \mu^E(s_{i+1}, s_i)) \\ &= \int \mu^{\pi_\theta}(s_T, \dots, s_0) \sum_{i=0..T-1} (\log \mu^{\pi_\theta}(s_{i+1}, s_i) \\ &\quad - \log \mu^E(s_{i+1}, s_i)) \\ &= \int \mu^{\pi_\theta}(s_T, \dots, s_0) \sum_{i=0..T-1} (\log \mu^{\pi_\theta}(s_{i+1} | s_i) \\ &\quad + \log \mu^{\pi_\theta}(s_i) - \log \mu^E(s_{i+1} | s_i) - \log \mu^E(s_i)) \\ &= \mathbb{E}_{(s_T, \dots, s_0) \sim \mu^{\pi_\theta}} \left[ \log \frac{\mu^{\pi_\theta}(s_T, \dots, s_0)}{\mu^E(s_T, \dots, s_0)} \right. \\ &\quad \left. + \log \prod_{i=1..T-1} \frac{\mu^{\pi_\theta}(s_i)}{\mu^E(s_i)} \right] \\ &= \mathbb{D}_{KL}(\mu^{\pi_\theta}(s_T, \dots, s_0) || \mu^E(s_T, \dots, s_0)) \\ &\quad + \sum_{i=1..T-1} \mathbb{E}_{(s_T, \dots, s_0) \sim \mu^{\pi_\theta}} \left[ \log \frac{\mu^{\pi_\theta}(s_i)}{\mu^E(s_i)} \right] \\ &= \mathbb{D}_{KL}(\mu^{\pi_\theta}(s_T, \dots, s_0) || \mu^E(s_T, \dots, s_0)) \\ &\quad + \sum_{i=1..T-1} \mathbb{D}_{KL}(\mu^{\pi_\theta}(s_i) || \mu^E(s_i)) \end{aligned} \quad (16)$$

### A.2 Bounded rewards

Since we use the SAC algorithm as a subroutine all rewards must be bounded. This is true if all subterms of our reward function

$$r(a_i, s_i) = \mathbb{E}_{s_{i+1} \sim \mu^{\pi_\theta}(s_{i+1} | s_i)} [-\log p(s_{i+1} | a_i, s_i) + \log \pi'_\theta(a_i | s_{i+1}, s_i) + \log \mu^E(s_{i+1} | s_i)] \quad (17)$$

are bounded which holds if

$$\epsilon \leq \pi'_\theta(a_i | s_{i+1}, s_i) p(s_{i+1} | a_i, s_i), \quad \mu^E(s_{i+1} | s_i) \leq H \quad \forall a_i, s_i, s_{i+1} \quad (18)$$

for some  $\epsilon$  and  $H$  which is a rather strong assumption which requires compact action and state spaces and a non-zero probability to reach every state  $s_{i+1}$  given any action  $a_i$  from a predecessor state  $s_i$ . Since this is in general not the case in practice we clip the logarithms of  $\pi'_\theta(a_i | s_{i+1}, s_i), p(s_{i+1} | a_i, s_i), \mu^E(s_{i+1} | s_i)$  to  $[-15, 1e9]$ . It should be noted that clipping the logarithms to a maximum negative value still provides a reward signal which guides the imitation learning to policies which achieve higher rewards.

### A.3 Correctness of using replay buffer

Here we argue that Algorithm 1 leads to a local optimum of the KLD objective from Equation 9 under the conditions: a) In the large sample limit per iteration b) appropriate density estimators and optimizers are used c) Equation 9 is minimized by optimizing the policy using a maximum entropy RL algorithm d) the inverse action policy  $\pi'(a | s', s)$  is trained using maximum likelihood from a replay buffer in an alternating fashion with the policy optimization.

In Section 3 we show that Equation 9 is a maximum entropy RL objective. Thus when optimizing the policy  $\pi_{\theta(e)}$  in episode  $e$  in Algorithm 1 using the maximum entropy RL algorithm SAC [Haarnoja *et al.*, 2018a] keeping the parameters of the conditional normalizing flows  $\mu^E(s' | s)$ ,  $\mu_\phi(s' | s, a)$ , and  $\mu_\eta(a | s', s)$  (to stay consistent with our method section, we use the distribution definitions here instead of the model definition) fixed which define the reward implies

$$\begin{aligned} &\sum_{i=0..T-1} \mathbb{E}_{(s_i, a_i, s_{i+1}) \sim \pi_{\theta(e)}} [\log p(s_{i+1} | a_i, s_i) \\ &\quad + \log \pi_{\theta(e)}(a_i | s_i) - \log \pi'_{\theta(e)}(a_i | s_{i+1}, s_i) \\ &\quad - \log \mu^E(s_{i+1} | s_i)] \\ &\leq \sum_{i=0..T-1} \mathbb{E}_{(s_i, a_i, s_{i+1}) \sim \pi_{\theta(e-1)}} [\log p(s_{i+1} | a_i, s_i) \\ &\quad + \log \pi_{\theta(e-1)}(a_i | s_i) - \log \pi'_{\theta(e)}(a_i | s_{i+1}, s_i) \\ &\quad - \log \mu^E(s_{i+1} | s_i)] \end{aligned} \quad (19)$$

Now, in the next episode  $e + 1$  the first part of Algorithm 1, i.e. optimizing the model of the inverse action policy  $\pi'_{\theta(e+1)}$  with a maximum likelihood objective using the new replay buffer data  $(s_i, a_i, s_{i+1}) \sim \pi_{\theta(e)}$  obtained from rollouts in episode  $e + 1$  with the new policy  $\pi_{\theta(e)}$  trained in episode  $e$  leads to

$$\begin{aligned} &\sum_{i=0..T-1} \mathbb{E}_{(s_i, a_i, s_{i+1}) \sim \pi_{\theta(e)}} [-\log \pi'_{\theta(e+1)}(a_i | s_{i+1}, s_i)] \\ &\leq \sum_{i=0..T-1} \mathbb{E}_{(s_i, a_i, s_{i+1}) \sim \pi_{\theta(e)}} [-\log \pi'_{\theta(e)}(a_i | s_{i+1}, s_i)] \end{aligned} \quad (20)$$

due to the maximum likelihood objective for the inverse action policy.



Using this inequality one obtains

$$\begin{aligned}
& \sum_{i=0..T-1} \mathbb{E}_{(s_i, a_i, s_{i+1}) \sim \pi_{\theta(e)}} [\log p(s_{i+1} | a_i, s_i) \\
& \quad + \log \pi_{\theta(e)}(a_i | s_i) - \log \pi'_{\theta(e+1)}(a_i | s_{i+1}, s_i) \\
& \quad - \log \mu^E(s_{i+1} | s_i)] \\
\leq & \sum_{i=0..T-1} \mathbb{E}_{(s_i, a_i, s_{i+1}) \sim \pi_{\theta(e-1)}} [\log p(s_{i+1} | a_i, s_i) \\
& \quad + \log \pi_{\theta(e-1)}(a_i | s_i) - \log \pi'_{\theta(e)}(a_i | s_{i+1}, s_i) \\
& \quad - \log \mu^E(s_{i+1} | s_i)] \tag{21}
\end{aligned}$$

Thus Algorithm 1 optimizes Equation 9 also in the "update dynamics models" part when training  $\mu_{\eta}(a | s', s)$  using maximum likelihood from a replay buffer. Thus, optimizing the policy  $\pi$  using SAC and training the model of the inverse action policy  $\pi'$  using the replay buffer and maximum likelihood are non-competing and non adversarial objectives, they alternately minimize the same objective in each part of Algorithm 1 and decrease the Kulback-Leibler Divergence in each step, ending in a minimum at convergence since the KLD is bounded by 0 from below.

The inequality from Equation 20 is based on the maximum likelihood objective and a "clean" replay buffer that contains only samples from the current policy. But it can be shown that it also holds for a replay buffer which contains a mixture of samples from the current and old policies: the inequality holds for the mixture distribution which contains a fraction  $\alpha$  of the replay buffer which stems from the new policy and a fraction  $1 - \alpha$  which stems from the old policies ( $\alpha$  depends on the size of the replay buffer and the number of new samples obtained in the current rollout). I.e.  $p(RB(e+1)) = \alpha \pi_{\theta(e+1)} + (1 - \alpha)p(RB(e))$ . Since the old inverse action policy  $\pi'_{\theta(e)}$  is the argmax of the maximum likelihood objective of the  $1 - \alpha$  fraction of RB(e+1) which is RB(e) it is better or equal than any other inverse action policy with regard to that previous replay buffer RB(e). Thus

$$\begin{aligned}
& \sum_{i=0..T-1} \mathbb{E}_{(s_i, a_i, s_{i+1}) \sim RB(e)} [-\log \pi'_{\theta(e+1)}(a_i | s_{i+1}, s_i)] \\
\geq & \sum_{i=0..T-1} \mathbb{E}_{(s_i, a_i, s_{i+1}) \sim RB(e)} [-\log \pi'_{\theta(e)}(a_i | s_{i+1}, s_i)] \tag{22}
\end{aligned}$$

due to the maximum likelihood objective for  $\pi'_{\theta(e+1)}$  on the data RB(e+1) the following inequality follows:

$$\begin{aligned}
& \sum_{i=0..T-1} \mathbb{E}_{(s_i, a_i, s_{i+1}) \sim RB(e+1)} [-\log \pi'_{\theta(e+1)}(a_i | s_{i+1}, s_i)] \\
\leq & \sum_{i=0..T-1} \mathbb{E}_{(s_i, a_i, s_{i+1}) \sim RB(e+1)} [-\log \pi'_{\theta(e)}(a_i | s_{i+1}, s_i)] \tag{23}
\end{aligned}$$

Also, by using the mixture definition of RB(e+1) one can

rewrite an Expectation over RB(e+1) as follows:

$$\begin{aligned}
\mathbb{E}_{(s_i, a_i, s_{i+1}) \sim RB(e+1)} [f] &= \alpha \mathbb{E}_{(s_i, a_i, s_{i+1}) \sim \pi_{\theta(e)}} [f] \\
& \quad + (1 - \alpha) \mathbb{E}_{(s_i, a_i, s_{i+1}) \sim RB(e)} [f] \tag{24}
\end{aligned}$$

Using the expanded Expectation Inequality 23 can be rewritten as follows:

$$\begin{aligned}
& \sum_{i=0..T-1} [\alpha \mathbb{E}_{(s_i, a_i, s_{i+1}) \sim \pi_{\theta(e)}} - \log \pi'_{\theta(e+1)}(a_i | s_{i+1}, s_i) \\
& \quad + (1 - \alpha) \mathbb{E}_{(s_i, a_i, s_{i+1}) \sim RB(e)} - \log \pi'_{\theta(e+1)}(a_i | s_{i+1}, s_i)] \\
\leq & \sum_{i=0..T-1} [\alpha \mathbb{E}_{(s_i, a_i, s_{i+1}) \sim \pi_{\theta(e)}} - \log \pi'_{\theta(e)}(a_i | s_{i+1}, s_i) \\
& \quad + (1 - \alpha) \mathbb{E}_{(s_i, a_i, s_{i+1}) \sim RB(e)} - \log \pi'_{\theta(e)}(a_i | s_{i+1}, s_i)] \tag{25}
\end{aligned}$$

By using Inequality 22 it can be rewritten to

$$\begin{aligned}
& \sum_{i=0..T-1} [\alpha \mathbb{E}_{(s_i, a_i, s_{i+1}) \sim \pi_{\theta(e)}} - \log \pi'_{\theta(e+1)}(a_i | s_{i+1}, s_i) \\
& \quad + (1 - \alpha) \mathbb{E}_{(s_i, a_i, s_{i+1}) \sim RB(e)} - \log \pi'_{\theta(e+1)}(a_i | s_{i+1}, s_i)] \\
\leq & \sum_{i=0..T-1} [\alpha \mathbb{E}_{(s_i, a_i, s_{i+1}) \sim \pi_{\theta(e)}} - \log \pi'_{\theta(e)}(a_i | s_{i+1}, s_i) \\
& \quad + (1 - \alpha) \mathbb{E}_{(s_i, a_i, s_{i+1}) \sim RB(e)} - \log \pi'_{\theta(e+1)}(a_i | s_{i+1}, s_i)] \tag{26}
\end{aligned}$$

which implies (by subtracting the common  $1 - \alpha$  term from both sides)

$$\begin{aligned}
& \sum_{i=0..T-1} [\alpha \mathbb{E}_{(s_i, a_i, s_{i+1}) \sim \pi_{\theta(e)}} - \log \pi'_{\theta(e+1)}(a_i | s_{i+1}, s_i) \\
\leq & \sum_{i=0..T-1} [\alpha \mathbb{E}_{(s_i, a_i, s_{i+1}) \sim \pi_{\theta(e)}} - \log \pi'_{\theta(e)}(a_i | s_{i+1}, s_i)] \tag{27}
\end{aligned}$$

which is Inequality 20 multiplied by  $\alpha$  and thus also implies (together with Inequality 19) Inequality 21. From this follows the convergence of Algorithm 1 to a minimum when using a mixed replay buffer.

#### A.4 Implementation Details

We use the same policy implementation for all our SOIL-TDM experiments. The stochastic policies  $\pi_{\theta}(a_t | s_t)$  are modeled as a diagonal Gaussian to estimate continuous actions with two hidden layers (512, 512) with ReLU nonlinearities.

To train a policy using SAC as the RL algorithm, we also need to model a Q-function. Our implementation of SAC is based on the original implementation from Haarnoja et al. [2018b] and the used hyperparameter are described in Table 1. In this implementation, they use two identical Q-Functions with different initialization to stabilize the training process. These Q-Functions are also modeled with an MLP having two hidden layers (512, 512) and Leaky ReLU. We kept the entropy parameter  $\alpha$  fixed to 1 and did not apply automatic entropy tuning as described by Haarnoja et al. [2018b].

We implement all our models for SOIL-TDM using the PyTorch framework version 1.9.0<sup>3</sup>. To estimate the imita-

<sup>3</sup><https://github.com/pytorch/pytorch>

Table 1: Training Hyperparameter

SAC Parameter	Value
Optimizer	Adam
learning rate policy	$1 \cdot 10^{-4}$
learning rate Q-function	$3 \cdot 10^{-4}$
discount $\gamma$ (Halfcheetah, Walker2D)	0.7
discount $\gamma$	0.9
mini batch size	2048
replay buffer size	$1 \cdot 10^5$
target update interval	1
number of environments	16
max number of environment steps	$4.0 \cdot 10^6$
SOIL-TDM Parameter	Value
expert transition model training steps	$10^3 - 10^4$
learning rate expert transition model	$1 \cdot 10^{-4}$
learning rate forward dynamics model	$1 \cdot 10^{-4}$
learning rate backward dynamics model	$1 \cdot 10^{-4}$
update interval dynamics models	1

tion reward in SOIL-TDM a model for the expert transitions  $\mu_E(s'|s)$  as well as a forward  $\mu_\phi(s'|s, a)$  and backward dynamics model  $\mu_\eta(a|s', s)$  has to be learned. All three density models are based on RealNVPs [Dinh *et al.*, 2017] consisting of several flow blocks where MLPs preprocess the conditions to a smaller condition size. The RealNVP transformation parameters are also calculated using MLPs, which process a concatenation of the input and the condition features. After each flow block, we added activation normalization layers like [Kingma and Dhariwal, 2018]. To implement these models, we use the publicly available VLL-FrEIA<sup>4</sup> framework version 0.2 [Ardizzone *et al.*, 2019] using their implementation of GLOWCouplingBlocks with exponent clamping activated. The setup for each model is layed out in Table 2. We add Gaussian noise to the state vector as a regularizer for the training of the expert transition model  $\mu_E(s'|s)$  which increased training stability for low amount of expert trajectories. We implement a linear decrease of the standard deviation from 0.05 to 0.005 during the training of the expert model.

We train and test all algorithms on a computer with 8 CPU cores, 64 GB of working memory and an RTX2080 Ti Graphics card. The compute time for the SOIL-TDM method depends on the time to convergence and is from 4h to 14h.

### A.5 Expert Data Generation and Baseline Methods

The expert data is generated by training an expert policy based on conditional normalizing flows and the SAC algorithm on the environment reward. A conditional normalizing flow policy has been chosen for the expert to make the

<sup>4</sup><https://github.com/VLL-HD/FrEIA> (Open Source MIT License)

Table 2: Normalizing Flow Setup

	$\mu^E(s' s)$	$\mu_\phi(s' s, a)$	$\mu_\eta(a s', s)$
N flow blocks	16	16	16
Condition hidden neurons	64	48	256
Condition hidden layer	2	2	2
Condition feature size	32	32	32
Flow block hidden neurons	64	48	256
Flow block hidden layer	2	2	2
Exponent clamping	6	1	1

distribution matching problem for the baseline methods and SOIL-TDM - which employ a conditional Gaussian policy - more challenging and more similar to real-world IL settings. The idea is that real-world demonstrations might be more complex and experiments using the same policy setup for the expert and the imitator might not well translate to real-world tasks.

The stochastic flow policy  $\pi_\theta(a_t|s_t)$  is based on RealNVPs [Dinh *et al.*, 2017] which have the same setup as the normalizing flow implementations used for  $\mu^E(s'|s)$ ,  $\mu_\phi(s'|s, a)$ , and  $\mu_\eta(a|s', s)$  also using N=16 GLOWCouplingBlocks. The state is processed as a condition with one MLP having a hidden size of 128. Each flow block has an additional fully connected layer to further process the condition to a small feature size of 8. Every flow block has 128 hidden neurons. Finally, each action is passed through a tanh layer as it is described in the SAC implementation. The log probability calculation was adapted accordingly [Haarnoja *et al.*, 2018b]. The final episode reward of the trained expert policy is in Table 3.

The expert trajectories are generated using the trained policy and saved as done by [Ho and Ermon, 2016]<sup>5</sup>. For the OPOLO<sup>6</sup> and F-IRL<sup>7</sup> baseline, the original implementations with the official default parameters for each environment are used. Only the loading of the expert data was changed to use the demonstrations of the previously trained normalizing flow policy. Since, no official code for FORM was publicly available, the FORM baseline was implemented based on our method. We changed the reward to use the state prediction effect model  $\mu_\phi^{\pi_\theta}(s'|s)$  as proposed by Jaegle *et al.* [2021]. Both effect models were implemented using the same implementation as for our expert transition model  $\mu^E(s'|s)$ . Training of the expert effect model  $\mu_\omega^E(s'|s)$  was performed offline with the same hyperparameter setup used for our expert transition model  $\mu^E(s'|s)$  (see Table 1 and Table 2). The policy optimization was done using the same SAC setup as for our method since FORM does not depend on a specific RL algorithm [Jaegle *et al.*, 2021]. We tested different setups for the entropy parameter  $\alpha$  and found that automatic entropy tuning as described by Haarnoja *et al.* [2018b] worked best.

For our experiment with unknown true environment reward

<sup>5</sup><https://github.com/openai/imitation> (Open Source MIT License)

<sup>6</sup><https://github.com/illidanlab/opolo-code> (Open Source MIT License)

<sup>7</sup><https://github.com/twni2016/f-IRL> (Open Source MIT License)

Table 3: Episode Reward of Expert Policy

Environment	Average Expert Episode Reward
AntBulletEnv-v0	2583
HalfCheetahBulletEnv-v0	2272
HopperBulletEnv-v0	2357
Walker2DBulletEnv-v0	1805
HumanoidBulletEnv-v0	2750

the following selection criteria are used. For "OPOLO est. reward" the estimated return based on the reward  $r(s, s') = -\log(1 - D(s, s'))$  with the state  $s$ , next state  $s'$  and the discriminator output  $D(s, s')$  is used. For "OPOLO pol. loss" the original OPOLO policy loss is used:

$$J(\pi_\theta, Q) = (1 - \gamma)\mathbb{E}_{s \sim S_0}[Q(s, \pi_\theta(s))] + \mathbb{E}_{(s, a, s') \sim R}[f(r(s, s')) + \gamma Q(s', \pi_\theta(s')) - Q(s, a)] \quad (28)$$

With the Q-Function  $Q$  and the  $f$ -divergence function. For both estimates the original OPOLO implementation was used. For FORM the convergence was estimated with the estimated return based on the reward:  $r_t = \log \mu_\omega^E(s'|s) - \log \mu_{\Phi}^{\pi_\theta}(s'|s)$  using the normalizing flow effect models. For F-IRL we use the implementation of Ni et al. [2020] for the estimate of the Jensen-Shannon divergence between state marginals of the expert and policy

$$\frac{1}{2} \int p(x) \log \frac{2p(x)}{p(x) + q(x)} + q(x) \log \frac{2q(x)}{p(x) + q(x)} dx.$$

## A.6 Ablation Study

In this section we want to investigate the influence of difference components for our proposed imitation learning setup. First we want to answer the question if learning additional backward and forward dynamics models to estimate the state transition KLD improves policy performance. We compare our proposed method SOIL-TDM to an approach where we train a policy only based on the log-likelihood of the expert defined by:

$$r_{abl}(s, s') = \log \mu^E(s'|s) \quad (29)$$

Using this reward the policy is optimized using SAC as described earlier. We call this simplified reward design approach "Ablation only Expert Model". By comparing the performance of this method to our approach, we can show that learning additional density models to estimate forward and backward dynamics leads to improved policy performance. The resulting rewards are plotted in Figure 3. The relative reward using this ablation method is much lower compared to SOIL-TDM. Only for a high amount of trajectories does this method reach expert-level performance.

We furthermore want to evaluate how the quality of the learned normalizing flows affects the overall algorithm performance. We therefore report the estimated test log-likelihood of the trained expert models  $\mu^E(s'|s)$  for different amount of expert trajectories using a separate test dataset with 20 unseen expert trajectories in table 4. The influence of the

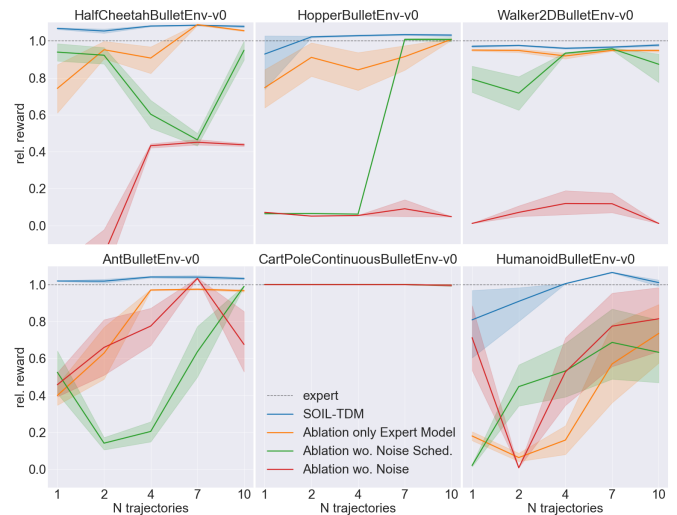


Figure 3: Best environment reward for ablation experiments. Relative reward for different amount of expert trajectories. The value 1 corresponds to expert policy performance.

Table 4: Test log-likelihood values of expert transition models  $\mu^E(s'|s)$  for 1, 2, 4, 7, and 10 training trajectories using 20 unknown test trajectories.

Environment	Log-Likelihood for $\mu^E(s' s)$
Ant	38.5, 43.5, 54.2, 59.9, 62.7
HalfCheetah	45.5, 47.8, 70.2, 71.1, 71.3
Hopper	14.4, 13.8, 15.9, 40.7, 36.9
Walker	38.9, 47.4, 62.5, 65.2, 67.4
Humanoid	39.5, 50.9, 62.9, 77.7, 77.4

Table 5: Test log-likelihood values of expert transition models  $\mu_{abl1}^E(s'|s)$  for 1, 2, 4, 7, and 10 training trajectories using 20 unknown test trajectories.

Environment	Log-Likelihood for $\mu_{abl1}^E(s' s)$ (constant noise)
Ant	30.9, 30.8, 41.1, 41.1, 59.0
HalfCheetah	26.3, 25.1, 78.3, 77.9, 79.2
Hopper	-31.6, -26.9, -24.1, 41.6, 40.8
Walker	42.1, 46.1, 55.8, 56.8, 58.1
Humanoid	26.4, 38.0, 51.5, 54.6, 57.4

Table 6: Test log-likelihood values of expert transition models  $\mu_{abl2}^E(s'|s)$  for 1, 2, 4, 7, and 10 training trajectories using 20 unknown test trajectories.

Environment	Log-Likelihood for $\mu_{abl2}^E(s' s)$ (no noise)
Ant	28.7, 31.9, 37.3, 37.4, 38.9
HalfCheetah	<i>-inf</i> , <i>-inf</i> , -270.2, -194.2, -187.8
Hopper	-171.3, -629.0, -379.1, -87.1, -70.9
Walker	<i>-inf</i> , <i>-inf</i> , -389.0, -182.4, -180.1
Humanoid	25.9, 36.7, 46.4, 50.1, 52.1

expert model quality on the overall algorithm performance can be seen by comparing the test log-likelihood to the reward of the trained policy (in Figure 3 "SOIL-TDM" for our method and "Ablation only Expert Model" for the simplified reward using the same expert model  $\mu^E(s'|s)$ ). SOIL-TDM is less sensitive to expert model performance compared to "Ablation only Expert Model".

Lastly, we want to investigate the expert model training. In the improved expert model training Routine, we regularize the optimization by adding Gaussian noise to the expert state values and linearly decrease its standard deviation down to 0.005 during training. As an additional ablation, we tested 2 different training setups for the expert transition models  $\mu^E(s'|s)$ . For the first model ( $\mu_{abl1}^E(s'|s)$ ) we omit the noise decay and only use the final constant Gaussian noise during training. For the second model ( $\mu_{abl2}^E(s'|s)$ ) no noise is added during training of the expert model. We evaluated also the test log-likelihood of the trained models using the test dataset with 20 unseen expert trajectories. The resulting test log-likelihoods are in Tables 5 - 6. The results show that, constant Gaussian noise already improves the performance of the expert model and our applied noise scheduling routine results in further performance improvements. We also used the trained expert models for policy training based on the ablation reward from Equation 29. These ablation methods are called "Ablation wo. Noise Sched.", "Ablation wo. Noise" respectively. The final rewards of these methods are also plotted in Figure 3. The results indicate that adding noise to the states during the offline training of the expert transition model also improves final policy performance.

## A.7 Additional Results

The following figures (Figure 4 - 8) show the policy loss and the estimated reward together with the environment reward during the training on different pybullet environments

for OPOLO, F-IRL, FORM, and SOIL-TDM (our method). All plots have been generated from training runs with 4 expert trajectories and 10 test rollouts. It can be seen that the estimated reward and policy loss from SOIL-TDM correlates well with the true environment reward. It is possible that the policy loss of SOIL-TDM is lower than 0 since its based not on the true distributions. Instead its based on learned and inferred estimates of expert state conditional distribution, policy state conditional distribution, policy inverse action distribution and q-function with relatively large absolute values ( $\sim 50 - 100$ ) each. These estimation errors accumulate in each time-step due to sum and subtraction and due to the Q-function also over (on average) 500 timesteps which can lead to relatively large negative values.

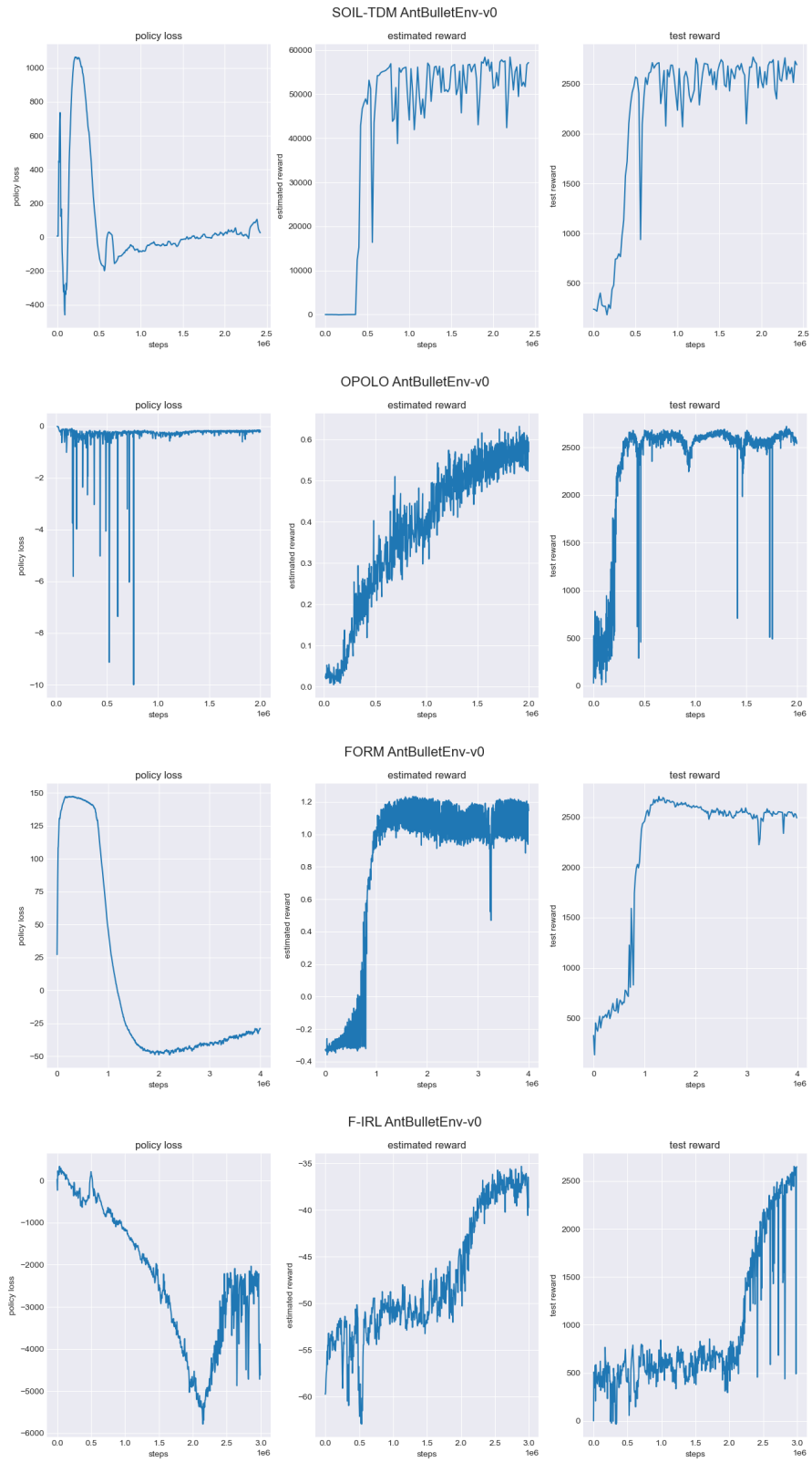


Figure 4: The policy loss, estimated reward and the environment test loss during training in the pybullet Ant environment using our proposed SOIL-TDM and the OPOLO, F-IRL, and FORM implementations with 4 expert trajectories.

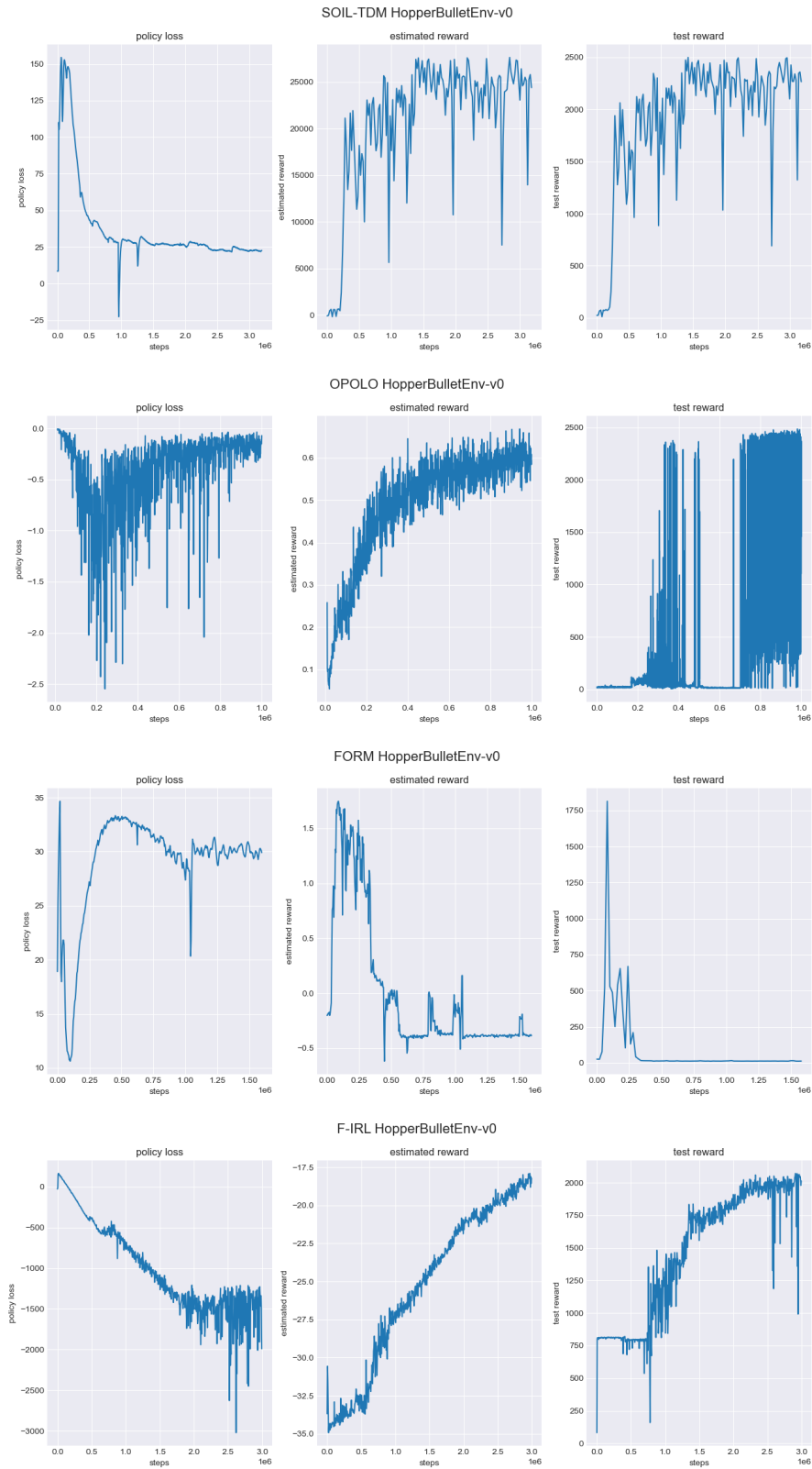


Figure 5: The policy loss, estimated reward and the environment test reward during training in the pybullet Hopper environment using our proposed SOIL-TDM and the OPOLO, F-IRL, and FORM implementations with 4 expert trajectories.

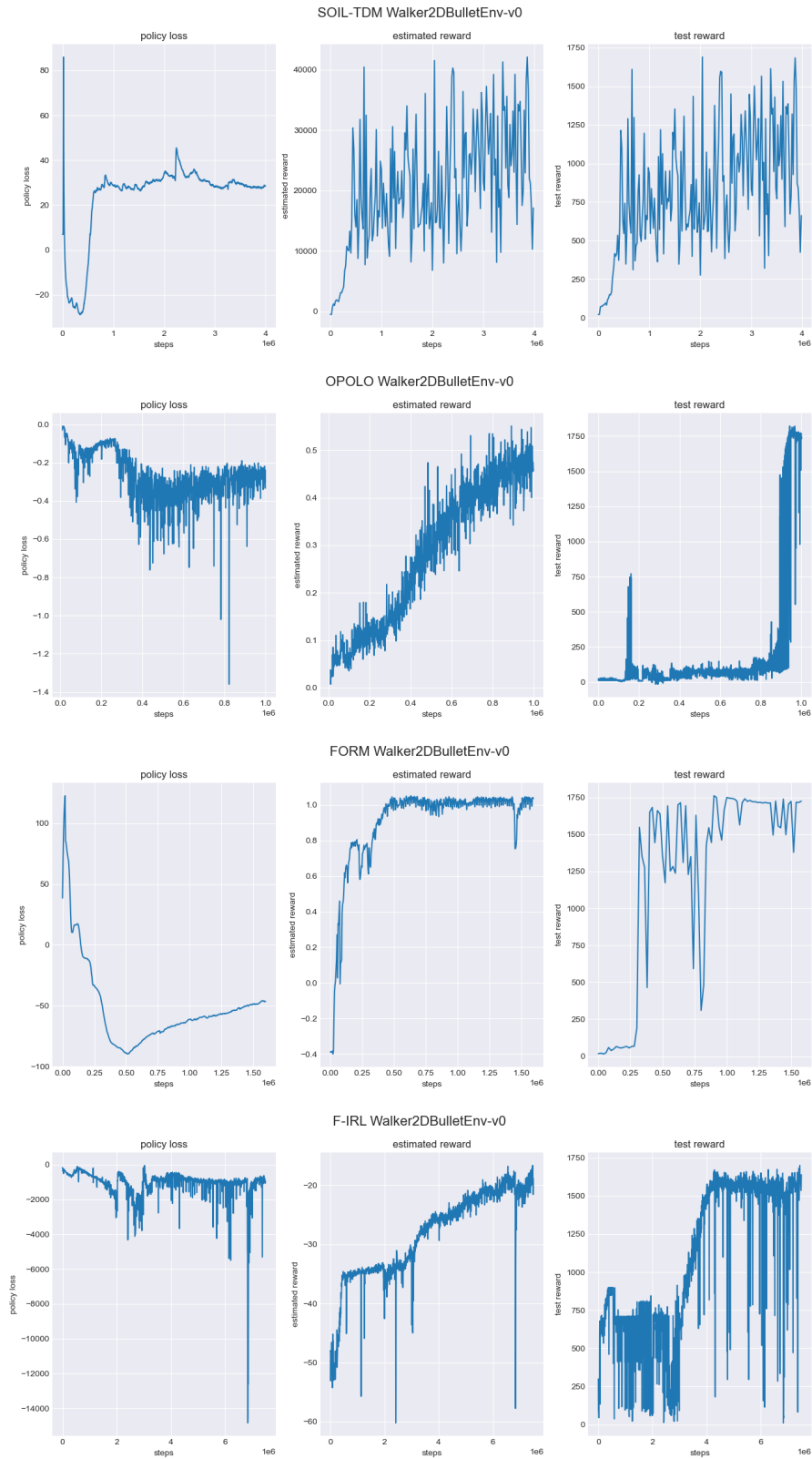


Figure 6: The policy loss, estimated reward and the environment test reward during training in the pybullet Walker2D environment using our proposed SOIL-TDM and the OPOLO, F-IRL, and FORM implementations with 4 expert trajectories.

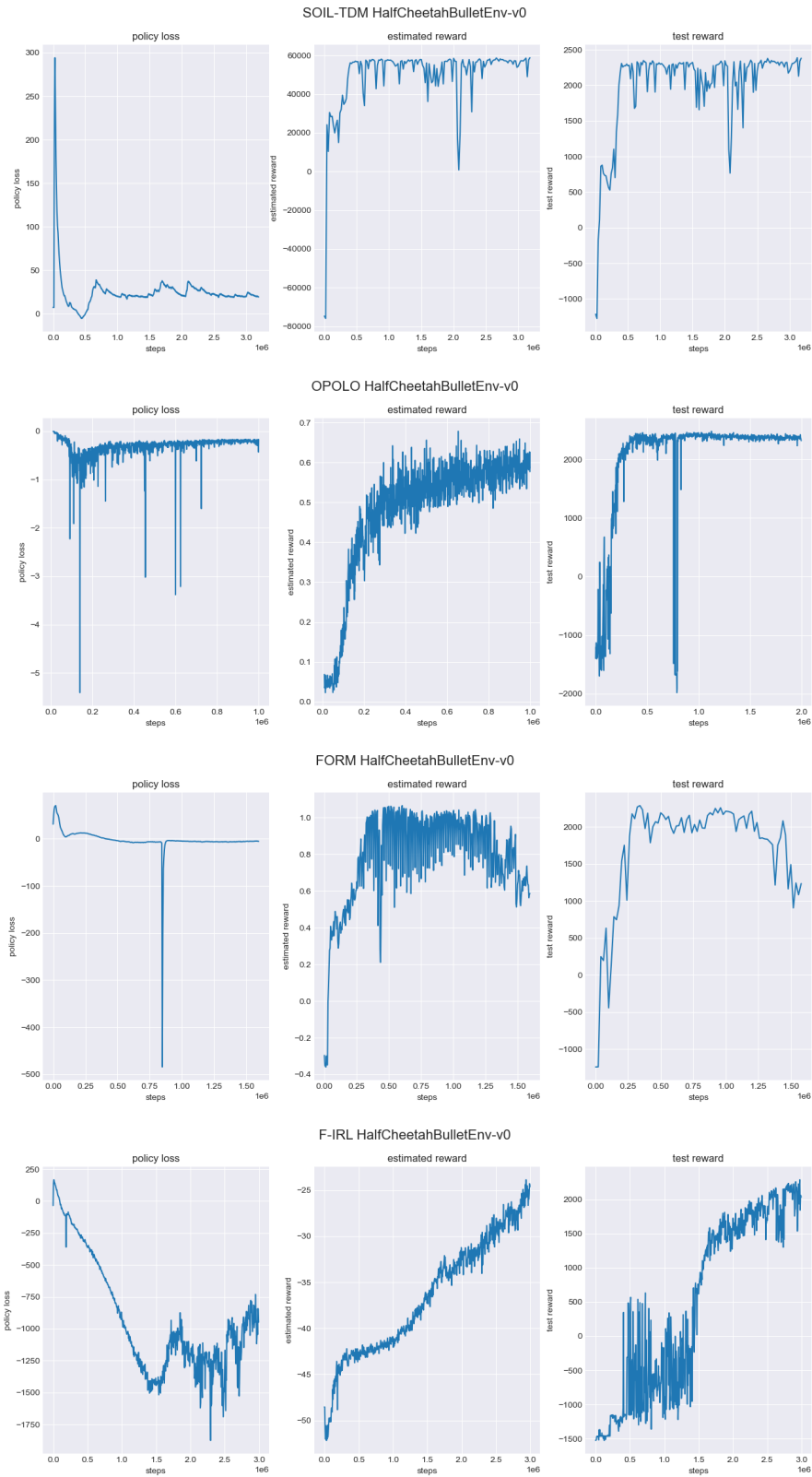


Figure 7: The policy loss, estimated reward and the environment test reward during training in the pybullet HalfCheetah environment using our proposed SOIL-TDM and the OPOLO, F-IRL, and FORM implementations with 4 expert trajectories.



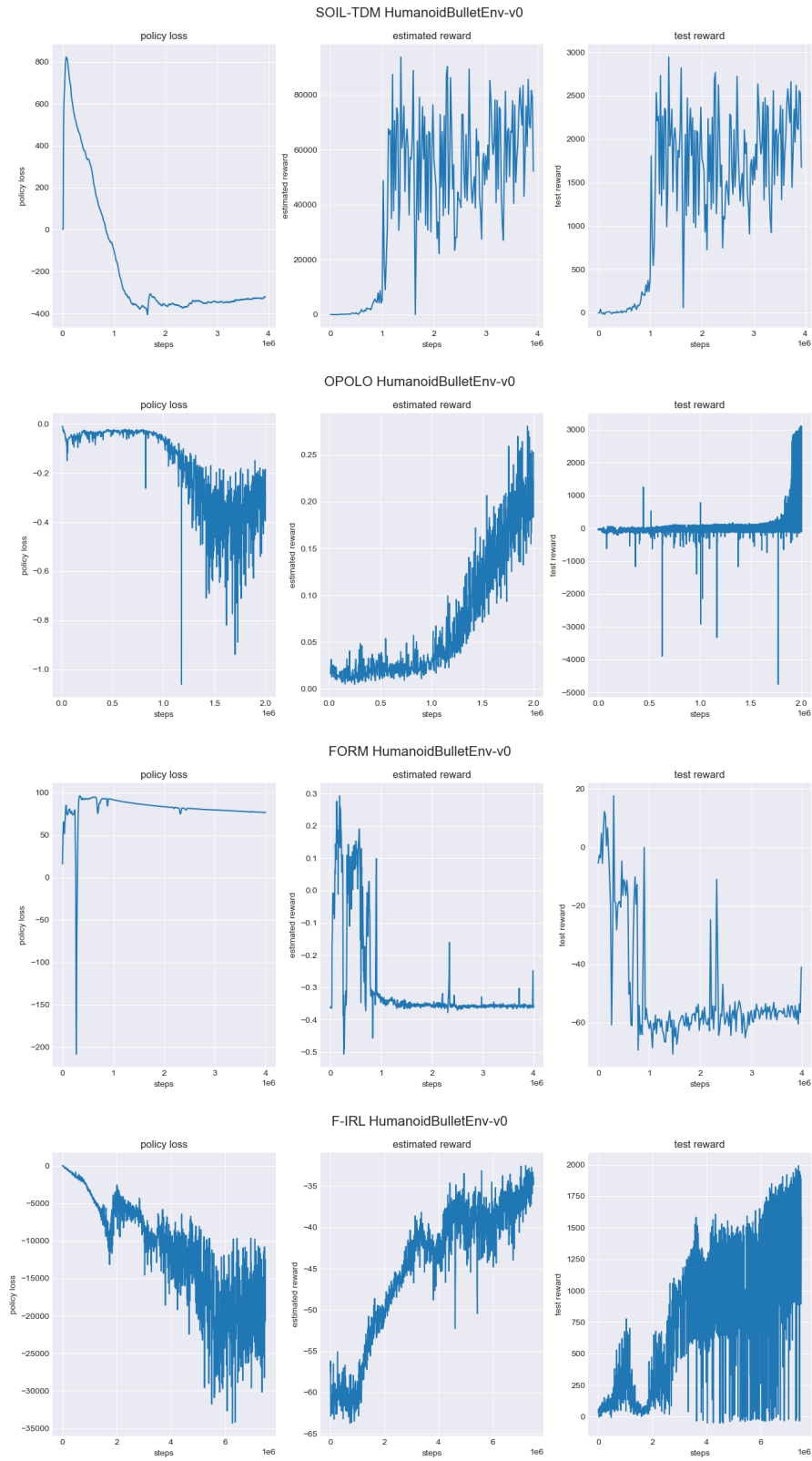


Figure 8: The policy loss, estimated reward and the environment test reward during training in the pybullet Humanoid environment using our proposed SOIL-TDM and the OPOLO, F-IRL, and FORM implementations with 4 expert trajectories.